

Asymptotic normalization coefficients from *ab initio* calculations

Kenneth M. Nollett* and R. B. Wiringa

Physics Division, Argonne National Laboratory, Argonne, IL 60439, USA

(Dated: November 25, 2018)

We present calculations of asymptotic normalization coefficients (ANCs) for one-nucleon removals from nuclear states of mass numbers $3 \leq A \leq 9$. Our ANCs were computed from variational Monte Carlo solutions to the many-body Schrödinger equation with the combined Argonne v_{18} two-nucleon and Urbana IX three-nucleon potentials. Instead of computing explicit overlap integrals, we applied a Green's function method that is insensitive to the difficulties of constructing and Monte Carlo sampling the long-range tails of the variational wave functions. This method also allows computation of the ANC at the physical separation energy, even when it differs from the separation energy for the Hamiltonian. We compare our results, which for most nuclei are the first *ab initio* calculations of ANCs, with existing experimental and theoretical results and discuss further possible applications of the technique.

PACS numbers: 21.10.Jx, 21.60.De, 02.70.Ss, 27.10.+h, 27.20.+n

Substantial experimental and theoretical effort over the past decade and a half has been expended on the extraction of asymptotic normalization coefficients (ANCs) from experiments involving light nuclei [1–9]. Most of this work has been motivated by the connection between ANCs and astrophysical cross sections, but ANCs also offer opportunities for significant new tests of *ab initio* nuclear calculations. In this Rapid Communication, we present predicted ANCs for several states of light nuclei up to $A = 9$, using the variational Monte Carlo (VMC) method and a realistic Hamiltonian.

Recent years have seen rapid advances in the *ab initio* theory of light nuclei [10–12]. Newly-available computing power has been brought to bear on the problem of computing properties of light ($A \lesssim 12$) nuclei from a new generation of accurate nucleon-nucleon and three-nucleon potentials. Many nuclear properties have been computed from the modern nuclear interactions, including charge radii, electroweak transition amplitudes, cross sections for scattering and radiative capture, and spectroscopic factors. Some ANCs have been computed [13–17], but there has been no systematic *ab initio* investigation of ANCs.

An ANC characterizes the asymptotic form of a nuclear overlap function, which is the projection of a nuclear wave function onto a product of subclusters. We consider only cases of one-nucleon removal, so the subclusters within a nucleus of mass A are the removed or “last” nucleon itself and a residual nucleus of mass $A - 1$. (Although we refer to the “last nucleon,” our wave functions are explicitly antisymmetric.) The overlap channel is further specified by orbital angular momentum l and its vector sum j with the spin of the last nucleon. The overlap function is then

$$R_{lj}^{J_{A-1}J_A}(r) \equiv \int \mathcal{A} \left[\Psi_{A-1}^{J_{A-1}} [\chi Y_l(\hat{\mathbf{r}})]_j \right]^\dagger \frac{\delta(r - r_{cc})}{r^2} \Psi_A^{J_A} d\mathbf{R}, \quad (1)$$

where $\Psi_A^{J_A}$ is the wave function of the mass- A nucleus with angular momentum J_A , $\Psi_{A-1}^{J_{A-1}}$ is a specific state

of the residual nucleus with angular momentum J_{A-1} , χ is the spin-isospin vector of the last nucleon, and r_{cc} is its separation from the center of mass of the other $A - 1$ nucleons. Square brackets denote angular momentum coupling, Y_l are spherical harmonics, and \mathcal{A} antisymmetrizes the product $\Psi_{A-1}^{J_{A-1}} \chi Y_l$ with respect to particle exchange. The integral extends over all particle coordinates $\mathbf{R} = (\mathbf{r}_1, \mathbf{r}_2, \dots, \mathbf{r}_A)$.

The form of the overlap as $r \rightarrow \infty$ is well known, because it satisfies a one-body Schrödinger equation including at most a Coulomb interaction. This form contains a Whittaker function $W_{-\eta m}$:

$$R_{lj}^{J_{A-1}J_A}(r \rightarrow \infty) = C_{lj}^{J_{A-1}J_A} W_{-\eta m}(2kr)/r, \quad (2)$$

with $\eta = \alpha Z_{A-1} Z_N \sqrt{\mu c^2 / 2B}$, α the fine-structure constant, Z_{A-1} and Z_N respectively the charges of the residual nucleus and the last nucleon, μ their reduced mass, B the separation energy of the last nucleon, $k = \sqrt{2\mu B} / \hbar$, and $m = l + 1/2$. (If the last nucleon is a neutron, then $Z_N = 0$ and $W_{-\eta m}(2kr) = \sqrt{2kr/\pi} K_m(kr)$, a modified spherical Bessel function of the third kind.) In the following, we omit the labels J_A and J_{A-1} for compactness of notation.

The only quantity in Eq. (2) that is not determined fully by the quantum numbers and the corresponding separation energy is the constant C_{lj} . It characterizes the overall scale of the long-range A -body wave function in the lj channel, and it is the ANC of that channel.

It can be shown that although the spectroscopic factor $S_{lj} \equiv \int R_{lj}^2(r) r^2 dr$ may depend strongly on the short-range potential and the choice of wave-function representation, the ANC as both a theoretically-computed and an experimentally-inferred quantity is less dependent on such details [18, 19]. Given reactions (e.g., well below the Coulomb barrier) that probe only the asymptotic part of R_{lj} , ANCs can be extracted from data with fewer assumptions than spectroscopic factors can.

Computing an ANC by direct integration of Eq. (1)

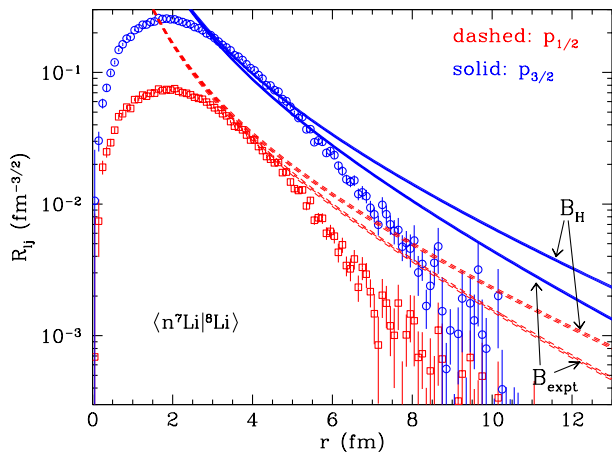


FIG. 1: (Color online) Points with Monte Carlo statistical errors show the $^8\text{Li} \rightarrow n^7\text{Li}$ overlap, computed from Eq. (1), of our VMC wave functions in $p_{1/2}$ (red squares) and $p_{3/2}$ (blue circles) channels. Curves with error bands show the asymptotic forms in Eq. (2), scaled by ANCs from Eq. (5). Dashed (red) curves are asymptotics for $p_{1/2}$ and solid (blue) ones are asymptotics for $p_{3/2}$. They are labeled “ B_H ” and “ B_{expt} ” according to the assumed neutron separation energies.

is problematic for most many-body methods. First, *ab initio* calculations may not yield the correct asymptotic form of Eq. (2). For example, methods using a harmonic-oscillator basis have basis functions with an asymptotic form $e^{-(r/b)^2}$, so that convergence to a long-range asymptotic form similar to e^{-kr} is slow. In variational methods, it is often difficult to construct a consistent set of correlations that has good long-range asymptotics while retaining short-range properties that are important for the variational energy. Second, the assumed Hamiltonian may not reproduce the experimental separation energy B_{expt} even when wave functions are computed exactly. Third, Monte Carlo methods suffer from the difficulty of finding a sampling scheme that samples the tails of Eq. (1) thoroughly while minimizing sample variance. All three difficulties are illustrated in Fig. 1.

There is another approach to computing ANCs that avoids all three of these difficulties, and versions of it have been derived in several contexts [20–23]. In this approach, explicit computation of the overlap function is replaced by an integral over the wave-function interior. The Schrödinger equation

$$(H - E)\Psi_A = 0 \quad (3)$$

that yields wave function Ψ_A with energy E may be rewritten as

$$\begin{aligned} \Psi_A = & -[T_{\text{rel}} + V_C + B]^{-1} (U_{\text{rel}} - V_C) \Psi_A \\ & - [T_{\text{rel}} + V_C + B]^{-1} (H_{\text{int}} - E_{\text{int}}) \Psi_A. \end{aligned} \quad (4)$$

We have broken up the Hamiltonian H into the relative kinetic energy T_{rel} between the residual nucleus and

last nucleon, a sum of terms H_{int} involving only nucleons within the residual nucleus, and a sum of terms U_{rel} involving the last nucleon. The point-Coulomb potential between the residual nucleus and last nucleon is $V_C = Z_{A-1}Z_N\alpha\hbar c/r_{cc}$. Similarly, $E = E_{\text{int}} - B$, with E_{int} being the purely internal energy of the residual nucleus.

If we rewrite the Green’s function $[T_{\text{rel}} + V_C + B]^{-1}$ in terms of special functions, project onto the product $[\Psi_{A-1}^{J_{A-1}} [\chi Y_l(\hat{\mathbf{r}})]_j]_{J_A}$ as in Eq. (1), take advantage of the identity that $(H_{\text{int}} - E_{\text{int}})\Psi_{A-1} = 0$, and take the $r \rightarrow \infty$ limit, we find that

$$\begin{aligned} C_{lj} = & \frac{2\mu}{k\hbar^2 w} \quad (5) \\ & \times \mathcal{A} \int \frac{M_{-\eta m}(2kr_{cc})}{r_{cc}} \Psi_{A-1}^\dagger \chi^\dagger Y_l^\dagger(\hat{\mathbf{r}}_{cc}) (U_{\text{rel}} - V_C) \Psi_A d\mathbf{R}. \end{aligned}$$

The integral extends over all particle coordinates, $M_{-\eta m}$ is the Whittaker function that is irregular at infinity, w is its Wronskian with the regular Whittaker function $W_{-\eta m}$, and the angular momentum algebra is omitted for simplicity.

The utility of Eq. (5) arises from the form of U_{rel} . If v_{ij} and V_{ijk} are respectively terms of the two- and three-body potentials involving nucleons labeled i, j , and k , and we always label the last nucleon A , then

$$U_{\text{rel}} = \sum_{i < A} v_{iA} + \sum_{i < j < A} V_{ijA}. \quad (6)$$

At large separation r_{cc} of the last nucleon, only the Coulomb terms of v_{iA} are nonzero. The monopole term of their sum is equal to V_C , so the factor $U_{\text{rel}} - V_C$ in Eq. (5) is short-ranged. In our calculations, it limits significant contributions to $r_{cc} < 7$ fm. Equation (5) thus reduces a problematic calculation involving the outer regions of Ψ_A to a manageable calculation involving its interior.

We implemented Eq. (5) within the VMC method described in Ref. [24]. The Hamiltonian comprised the Argonne v_{18} two-nucleon [25] and Urbana IX three-nucleon interactions [26]. For this interaction (AV18+UIX) we constructed variational wave functions Ψ_A and Ψ_{A-1} that minimize the energy expectation values while constraining them to give approximately correct charge radii, as determined experimentally (where known) or by exact Green’s function Monte Carlo (GFMC) calculations. The ANC integral was performed by Monte Carlo integration, using the same sampling scheme (with weight proportional to $|\Psi_A|^2$) as our energy calculations.

The distribution in r_{cc} of the ANC integrand is shown in Fig. 2 for the specific case of $^8\text{Li} \rightarrow n^7\text{Li}$. (Where there is no further label, the ground state of a nucleus is implied). It may be seen that the ANC integral is contained entirely within about 7 fm. The distribution of Monte Carlo samples, shown as a dotted curve, is broadly similar to the distribution of the ANC integrand, so the

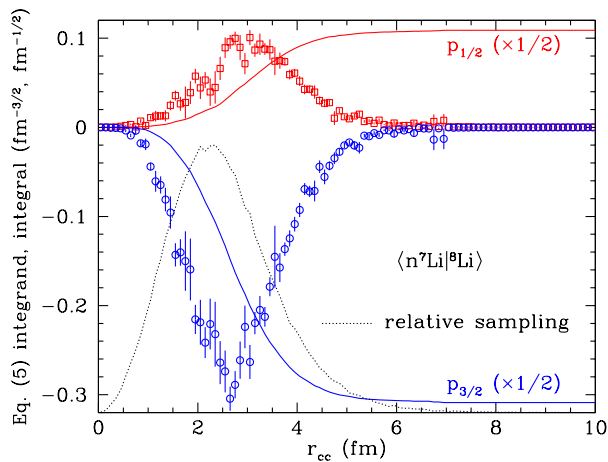


FIG. 2: (Color online) The integrand of Eq. (5) ($\times 2\mu/k\hbar\omega$) is shown for the $p_{1/2}$ (red squares) and $p_{3/2}$ (blue circles) neutrons in ${}^8\text{Li} \rightarrow n\text{Li}$. It is binned by the $n\text{-}{}^7\text{Li}$ separation r_{cc} with bars showing Monte Carlo errors. The solid curves are cumulative integrals of Eq. (5), starting from the origin; at large r_{cc} , they are the ANCs (divided by 2 for visibility on this scale). The dotted curve with no scale shows the distribution of Monte Carlo samples.

integral is computed with relatively small statistical errors.

The computed C_{ij} depend sensitively on the separation energies B . Equation (5) contains B implicitly through $k = \sqrt{2\mu B}/\hbar$ and $\eta \propto 1/\sqrt{B}$, and it is rigorously true when $B = E_{\text{int}} - E$ for the given potential. However, there are often significant differences between this B and the experimental separation energy B_{expt} . We computed several ANCs in light nuclei, first using the GFMC B_H for the AV18+UIX Hamiltonian and then using B_{expt} .

The use of B_{expt} in Eq. (5) may be understood by considering small changes to the potential. When $B \ll |E|$, they can produce small changes in the wave-function interior but large fractional changes in B . The short-range part of the variational wave function derived from AV18+UIX is, therefore, similar to the solution that would be obtained from a slightly different potential tuned (e.g. with small extra terms) so that $B_H = B_{\text{expt}}$. Inserting a $k \propto \sqrt{B_{\text{expt}}}$ into Eq. (5) matches a wave-function interior approximating the true wave function onto the asymptotic form corresponding to B_{expt} . Instructive illustrations of this general principle, applied to much simpler wave functions, may be found in Ref. [27].

The use of Eq. (5) to compute asymptotic overlaps is demonstrated in Fig. 1, where ${}^8\text{Li} \rightarrow n\text{Li}$ overlaps computed directly from Eq. (1) are plotted next to $C_{ij}W_{-\eta m}/r$ from Eq. (5). It can be seen that the $W_{-\eta m}$ corresponding to $B_H = 1.3$ MeV [28] are rather different from those for $B_{\text{expt}} = 2.03$ MeV, though both energies are small fractions of the 41.3 MeV total binding energy for ${}^8\text{Li}$.

For both B values, the asymptotic R_{ij} match the short-

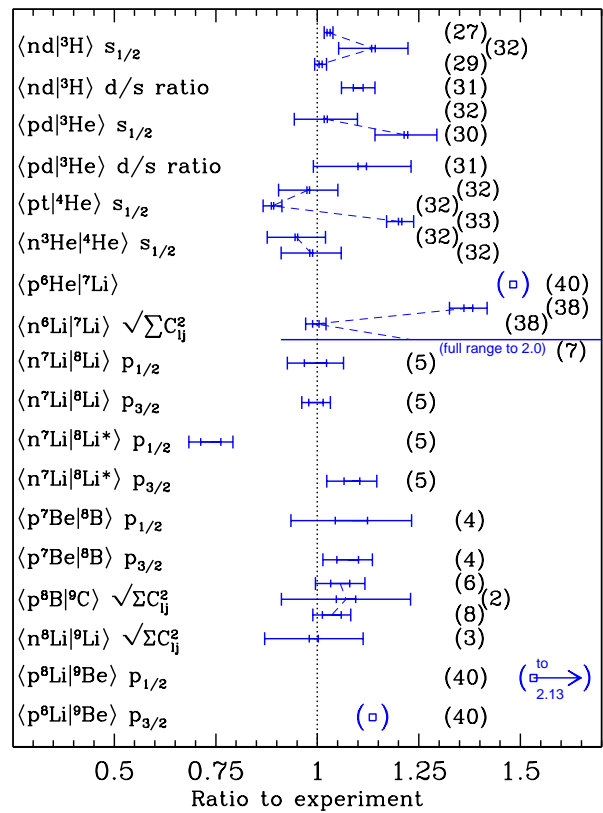


FIG. 3: (Color online) Predicted ANCs from Eq. (5), divided by experimentally-derived values from the references given at the right (those not appearing elsewhere are Refs. [29–31]). For each ANC, small error bars indicate the Monte Carlo error of Table I and larger error bars indicate its quadrature sum with the experimental error. Results for the same computed ANC divided by different “experimental” numbers are joined with dashed lines. Parentheses indicate particularly uncertain experimental constraints.

range overlaps at ~ 4 fm, where the ANC integral starts to converge. Use of B_H yields $C_{p1/2}^2 = 0.029(2)$ fm $^{-1}$ and $C_{p3/2}^2 = 0.237(9)$ fm $^{-1}$, compared with the respective values $0.048(6)$ fm $^{-1}$ and $0.384(38)$ fm $^{-1}$ from a transfer-reaction study [5]. The match between the computed and “measured” results is poor. Using B_{expt} yields $0.048(3)$ fm $^{-1}$ and $0.382(14)$ fm $^{-1}$, in very good agreement with experiment. This pattern of agreement with experiment for B_{expt} but disagreement for B_H repeats in all cases of substantial difference between B_H and B_{expt} . In the following, we consider only ANCs computed from B_{expt} , and we assign uncertainties based entirely on Monte Carlo statistics rather than (difficult) assessments of the variational wave functions. Limited testing with variant wave functions suggests that the total uncertainty is not much larger than the statistical uncertainties.

Our results are shown in Table I and compared with experimentally-derived numbers (where available) in Fig. 3. The lowest three sections of Table I re-

TABLE I: ANCs computed from Eq. (5) for given A -body nuclei, $(A - 1)$ -body residual nuclei, and angular momentum channels l_j or ^{2s+1}l . Units are $\text{fm}^{-1/2}$, and f -wave ANCs have been multiplied by 10^3 . Error estimates reflect Monte Carlo statistics only, and columns left empty are zero by exact symmetries. Asterisks denote first excited states.

A	$A - 1$	$s_{1/2}$	$d_{3/2}$	$C_{d3/2}/C_{s1/2}$	
^3H	^2H	2.127(8)	-0.0979(9)	-0.0460(5)	
^3He	^2H	2.144(8)	-0.0927(10)	-0.0432(5)	
^4He	^3H	-6.55(2)			
^4He	^3He	6.42(2)			
A	$A - 1$	$p_{1/2}$	$p_{3/2}$	$f_{5/2} \times 10^3$	$f_{7/2} \times 10^3$
^7Li	^6He		3.68(5)		
$^7\text{Li}^*$	^6He	3.49(5)			
^7Li	^6Li	1.652(12)	1.890(13)	-78(20)	
$^7\text{Li}^*$	^6Li	-0.543(16)	-2.54(4)		
^7Be	^6Li	-1.87(3)	-2.15(3)	63(9)	
$^7\text{Be}^*$	^6Li	0.559(16)	2.59(5)		
^8Li	^7Li	0.218(6)	-0.618(11)	5.2(5)	-2.5(15)
$^8\text{Li}^*$	^7Li	-0.090(3)	0.281(5)	-0.6(2)	
^8B	^7Be	0.246(9)	-0.691(17)	1.1(2)	-1.1(5)
^9C	^8B	-0.309(7)	1.125(12)	1.9(5)	-0.5(18)
^9Li	^8Li	0.308(7)	-1.140(13)	-4.1(10)	5(3)
^9Li	$^8\text{Li}^*$	-0.122(3)	0.695(7)	-1.1(6)	
^9Li	^8He		-5.99(8)		
^9Be	^8Li	5.03(6)	9.50(11)	35(34)	257(112)
^9Be	$^8\text{Li}^*$	6.56(5)	-6.21(7)	364(40)	
A	$A - 1$	2p	4p	$^2f \times 10^3$	$^4f \times 10^3$
^7Li	^6Li	2.510(18)	0.029(18)		-78(20)
$^7\text{Li}^*$	^6Li	-2.57(5)	-0.33(3)		
^7Be	^6Li	-2.85(4)	-0.04(4)		-63(9)
$^7\text{Be}^*$	^6Li	2.63(5)	0.34(3)		
^9Li	$^8\text{Li}^*$	-0.599(7)	-0.373(7)		1.1(6)
^9Be	$^8\text{Li}^*$	-0.25(9)	-9.03(8)		-364(40)
A	$A - 1$	4p	6p	$^4f \times 10^3$	$^6f \times 10^3$
^9C	^8B	0.868(14)	0.779(12)	0.1(19)	-2(1)
^9Li	^8Li	-0.882(15)	-0.785(12)	3.3(34)	5.2(19)
^9Be	^8Li	10.75(12)	-0.25(10)	256(117)	42(65)
A	$A - 1$	3p	5p	$^3f \times 10^3$	$^5f \times 10^3$
^8Li	^7Li	-0.283(12)	-0.591(12)	-0.3(16)	-5.8(10)
$^8\text{Li}^*$	^7Li	0.220(6)	0.197(5)		0.6(2)
^8B	^7Be	-0.315(19)	-0.662(19)	-0.6(5)	-1.4(4)

peat information from the second section, but in “channel spin” coupling of the form $[[J_{A-1} \frac{1}{2}]_s l]_{J_A}$ instead of $[J_{A-1} [l \frac{1}{2}]_j]_{J_A}$. We examined most channels up to $A = 9$ with either the A -body or the residual nucleus in its ground state and with both stable against particle decay. We now comment briefly on the comparison of our results with past work. Extensive discussions of past experimental and theoretical estimates may be found in Refs. [27, 32].

The s -wave ANCs for $A \leq 4$ nuclei have typically been inferred from cross sections using techniques based on analyticity of the scattering amplitude [32, 33], mostly thirty or more years ago. Although our ANCs agree with many of those results, Fig. 3 demonstrates the considerable systematic uncertainties of those methods discussed in Refs. [32, 34].

ANCs of ^3H and ^3He have been computed previously from modern realistic interactions using Eq. (5) [15] and were the focus of much activity following the development of Faddeev methods [34–36]. Particular emphasis was

placed on the ratio $C_{d3/2}/C_{s1/2}$, most precisely inferred from tensor analyzing powers [36]; those results are in reasonable agreement with ours.

The Pisa group has computed ANCs for $A \leq 4$ [15, 16] with AV18+UIX. Their $A = 3$ $C_{s1/2}$ are within 0.5% of ours, but their $C_{d3/2}/C_{s1/2}$ are 10% smaller. Their ^4He ANCs are also about 6% smaller than ours. The reason for this difference is unclear; it could reflect shortcomings of the variational wave functions, which miss the true AV18+UIX binding energy by 850 keV in ^4He . Ongoing work to compute overlaps using essentially exact wave functions from the GFMC method seems to support our values of the $A = 4$ ANCs [37]. (Nuclei with $A = 3, 4$ have substantially identical ANCs for B_H and B_{expt} because the AV18+UIX interaction was tuned to have $B_H \simeq B_{\text{expt}}$ in these systems. Pisa ANCs converted to our conventions may be found in Ref. [27].)

For $A > 4$ ANCs, experimental constraints have been inferred almost entirely from transfer [1–5, 7, 9, 38], knockout [8], or breakup [6] reactions, and are of generally more recent vintage than the $A \leq 4$ ANCs. In some cases components of different j contribute indistinguishably to differential cross sections, which then constrain only the sum $\sum_j C_{ij}^2$. These cases are indicated in Fig. 3 and shown as the square root of the sum for comparability of error bars. Our p -shell ANCs are in broadly good agreement with those inferred from experiment, particularly for the well-measured $A = 8$ ground state ANCs as discussed above. (Our calculations for $A = 8$ also agree with prior theoretical estimates of [17, 39].) Reference [27] presented many ANCs computed by applying Eq. (5) with a simpler potential to harmonic-oscillator wave functions derived from shell models; about half of our p -shell ANCs disagree with those calculations by more than 25%.

The most significant differences from previous work are in the $^7\text{Li} \rightarrow n^6\text{Li}$ ANCs. The comparison with experiment here is difficult because of the wide range of estimates, which extend from $\sqrt{\sum C_{ij}^2} = 1.26$ to $2.82 \text{ fm}^{-1/2}$ just from (d, t) at varying energy ([7], with full range shown in Fig. 3) and include other values within that range [38, 40]. The effective ANC of Huang et al. [41], whose capture model successfully matches $^6\text{Li}(p, \gamma)^7\text{Be}$ data, is 25% below ours.

The theoretical ANCs for $^7\text{Li} \rightarrow n^6\text{Li}$ (from a simpler model) in Ref. [27] are 20% to 40% smaller than ours. As with ^4He , ongoing GFMC work (with an improved three-body interaction) seems to support our results [37]. We also disagree with earlier integral-method predictions of the ratio of $^7\text{Be} \rightarrow p^6\text{Li}$ to isospin-mirror $^7\text{Li} \rightarrow n^6\text{Li}$ ANCs [42], finding 1.15 instead of 1.05 (though we agree with their 1.12 as the ratio of ^8B to ^8Li ANCs). The sources of these differences are unclear.

Table I includes ANCs for both p - and f -wave channels of p -shell nuclei. The small f -wave components arise

from the tensor terms the Hamiltonian, analogously to the d -wave components in s -shell nuclei [43]. We are unaware of any previous calculations of f -wave ANC's or attempts to measure them. A DWBA calculation of tensor analyzing powers in sub-Coulomb $^{208,209}\text{Pb}(^7\text{Li}, ^6\text{Li})X$ (analogous to triton d/s ratio experiments) suggests that both cross sections and analyzing powers may be too small to allow measurement of the f/p ratio [28]. Nonetheless, the f -wave ANC's demonstrate something of the power of the integral method: Within the VMC approach, computing ANC's for these small-amplitude channels from Eq. (1) would require far more computing time to achieve the same statistical accuracy, even if our variational wave functions guaranteed the correct asymptotic form.

Several extensions of this technique within the context of quantum Monte Carlo methods suggest themselves. The overlaps need not correspond only to one-nucleon removal, but may include cluster overlaps like $^4\text{He} \rightarrow dd$ and $^7\text{Be} \rightarrow \alpha^3\text{He}$. A straightforward extension of the definition of ANC's to include unbound states allows the prediction of energy widths from the integral method [44–46]. The ANC integral can also be evaluated within the GFMC method, which provides essentially exact results for a given potential. Use of the (computationally more demanding) Illinois three-body potentials [47] to generate the wave function and/or the ANC kernel will provide more accurate ANC's and B_H closer to B_{expt} . Finally, use of Eq. (4) away from the $r \rightarrow \infty$ limit should allow more accurate calculations of overlaps at all radii [20, 21, 27, 48].

We acknowledge useful discussions with I. Brida, S. C. Pieper, A. M. Mukhamedzhanov, H. Esbensen, and C. R. Brune. This work was supported by the U.S. Department of Energy, Office of Nuclear Physics, under contract No. DE-AC02-06CH11357. Calculations were performed on the Fusion computing cluster operated by the Laboratory Computing Resource Center at Argonne.

* Electronic address: nollett@anl.gov

- [1] A. Azhari et al., Phys. Rev. C **63**, 055803 (2001).
- [2] D. Beaumel et al., Phys. Lett. B **514**, 226 (2001).
- [3] B. Guo et al., Nucl. Phys. A **761**, 162 (2005).
- [4] G. Tabacaru et al., Phys. Rev. C **73**, 025808 (2006).
- [5] L. Trache et al., Phys. Rev. C **67**, 062801 (2003).
- [6] L. Trache et al., Phys. Rev. C **66**, 035801 (2002).
- [7] I. R. Gulamov, A. M. Mukhamedzhanov, and G. K. Nie, Phys. At. Nucl. **58**, 1689 (1995), Yad. Fiz. **58**, 1789 (1995).
- [8] J. Enders et al., Phys. Rev. C **67**, 064301 (2003).
- [9] A. Azhari et al., Phys. Rev. Lett. **82**, 3960 (1999).
- [10] S. C. Pieper and R. B. Wiringa, Annu. Rev. Nucl. Part. Sci. **51**, 53 (2001).
- [11] S. C. Pieper, Nuovo Cimento Rivista **31**, 709 (2008), arXiv:0711.1500.
- [12] P. Navrátil et al., J. Phys. G **36**, 083101 (2009).
- [13] K. M. Nollett, Phys. Rev. C **63**, 054002 (2001).
- [14] K. M. Nollett, R. B. Wiringa, and R. Schiavilla, Phys. Rev. C **63**, 024003 (2001).
- [15] A. Kievsky et al., Phys. Lett. B **406**, 292 (1997).
- [16] M. Viviani, A. Kievsky, and S. Rosati, Phys. Rev. C **71**, 024006 (2005).
- [17] P. Navrátil, C. A. Bertulani, and E. Caurier, Phys. Rev. C **73**, 065801 (2006).
- [18] J. L. Friar, Phys. Rev. C **20**, 325 (1979).
- [19] A. M. Mukhamedzhanov and A. S. Kadyrov, Phys. Rev. C **82**, 051601 (2010).
- [20] W. Pinkston and R. Satchler, Nucl. Phys. A **72**, 641 (1965).
- [21] M. Kawai and K. Yazaki, Prog. Theor. Phys. **37**, 638 (1967).
- [22] D. R. Lehman and B. F. Gibson, Phys. Rev. C **13**, 35 (1976).
- [23] A. M. Mukhamedzhanov and N. K. Timofeyuk, Sov. J. Nucl. Phys. **51**, 431 (1990), Yad. Fiz. **51**, 679 (1990).
- [24] R. B. Wiringa, AIP Conf. Proc. **1128**, 1 (2009).
- [25] R. B. Wiringa, V. G. J. Stoks, and R. Schiavilla, Phys. Rev. C **51**, 38 (1995).
- [26] B. S. Pudliner et al., Phys. Rev. Lett. **74**, 4396 (1995).
- [27] N. K. Timofeyuk, Phys. Rev. C **81**, 064306 (2010).
- [28] S. C. Pieper, (private communication).
- [29] B. A. Girard and M. G. Fuda, Phys. Rev. C **19**, 583 (1979).
- [30] A. V. Blinov et al., J. Phys. G. **11**, 623 (1985).
- [31] J. E. Purcell et al., Nucl. Phys. A **848**, 1 (2010).
- [32] M. P. Locher and T. Mizutani, Phys. Rep. **46**, 43 (1978).
- [33] L. D. Blokhintsev, I. Borbely, and E. I. Dolinskii, Sov. J. Part. Nucl. **8**, 485 (1977), Fiz. Elem. Chastits At. Yadra **8**, 1189 (1977).
- [34] J. L. Friar et al., Phys. Rev. C **37**, 2859 (1988).
- [35] H. R. Weller and D. R. Lehman, Annu. Rev. Nucl. Part. Sci. **38**, 563 (1988).
- [36] E. A. George and L. D. Knutson, Phys. Rev. C **48**, 688 (1993).
- [37] I. Brida, private communication.
- [38] S. A. Goncharov et al., Czech. J. Phys. **37**, 168 (1987).
- [39] D. Halderson, Phys. Rev. C **69**, 014609 (2004).
- [40] M. S. Bekbaev et al., Sov. J. Nucl. Phys. **54**, 232 (1991), Yad. Fiz. **54**, 387 (1991).
- [41] J. T. Huang, C. A. Bertulani, and V. Guimarães, At. Data Nuc. Data Tables **96**, 824 (2010).
- [42] N. K. Timofeyuk, R. C. Johnson, and A. M. Mukhamedzhanov, Phys. Rev. Lett. **91**, 232501 (2003).
- [43] A. M. Eiro and F. D. Santos, J. Phys. G **16**, 1139 (1990).
- [44] A. M. Mukhamedzhanov and R. E. Tribble, Phys. Rev. C **59**, 3418 (1999).
- [45] H. Esbensen and C. N. Davids, Phys. Rev. C **63**, 014315 (2000).
- [46] S. G. Kadmenskiĭ and V. G. Khlebstroev, Sov. J. Nucl. Phys. **18**, 505 (1974), Yad. Fiz. **18**, 980 (1973).
- [47] S. C. Pieper et al., Phys. Rev. C **64**, 014001 (2001).
- [48] A. M. Mukhamedzhanov et al., Sov. J. Nucl. Phys. **52**, 452 (1990), Yad. Fiz. **52**, 704 (1990).